Supporting Information

Robust, Brighter Red Emission from $CsPbI_3$ Perovskite Nanocrystals via Endotaxial Protection

*G. Krishnamurthy Grandhi[1], N. S. M. Viswanath[2], Jun Hyeong In[1], Han Bin Cho[1] and Won Bin Im[1,] **

[1]Division of Materials Science and Engineering, Hanyang University, 222 Wangsimni-ro, Seongdong-gu, Seoul, 04763, Republic of Korea

[2]School of Materials Science and Engineering, Chonnam National University, 77 Yongbong-ro, Buk-gu, Gwangju, 61186, Republic of Korea

*E-mail: imwonbin@hanyang.ac.kr

Experimental section

Materials

Cs_2CO_3, 1-octadecene (ODE), oleic acid (OlAc), lead bromide ($PbBr_2$), lead iodide (PbI_2), lead chloride ($PbCl_2$), hydrogen bromide (HBr), hydrogen chloride (HCl), hydrogen iodide (HI), and hexane were obtained from Sigma-Aldrich. Oleylamine (OlAm) was obtained from Hansol chemicals. All these chemicals were used without any further purification.

A light-yellowish and transparent Cs-oleate precursor was prepared by heating a mixture of Cs_2CO_3 (2.2 g) and OlAc (19.24 g) at 130 °C in a vacuum.

Synthesis of $CsPbI_3$-Cs_4PbI_6 NCs

PbI_2 (29 mg, ~0.06 mmol), ODE (5 mL), OlAc (0.5 mL), OlAm (0.5–0.65 mL), and HI (40 µL) were degassed in a 100-mL three-necked flask for about one hour at 120 ^oC. This was followed by the injection of Cs-oleate (0.3-0.4 mL) at 155 °C in an Ar atmosphere. After 5-10 s of this injection, the reaction was quenched in an ice-bath. The obtained NCs were centrifuged at 7000 rpm for 5 min. The supernatant was discarded, and 5 mL of hexane was added to the precipitate. The obtained hexane solution was then centrifuged at 5000 rpm for 5 min. The supernatant was stored and used for various measurements and experiments. While the use of 0.65 mL of OlAm and 0.4 mL of Cs-oleate during the synthesis led to the formation of $CsPbI_3$-Cs_4PbI_6 NCs with 1–2% $CsPbI_3$ phase fraction, employing 0.5 mL of OlAm and 0.3 mL of Cs-oleate produced $CsPbI_3$-Cs_4PbI_6 NCs with 6% $CsPbI_3$ phase fraction.

Synthesis of $CsPbBr_3$-Cs_4PbBr_6 hybrid NCs

Green-emitting and blue-emitting hybrid NCs were obtained by replacing PbI_2 and HI in the above synthesis procedure with $PbBr_2$ (~24 mg) and 24 µL of HBr, and $PbCl_2$ (~16.7 mg) and 24 µL of HCl, respectively.

Characterization techniques

The structure and size determination of the NCs were carried out using X-ray diffraction (XRD) technique and transmission electron microscopy (TEM). High-resolution XRD patterns of the NC films were recorded on Rigaku high resolution X-Ray diffractometer (model: SmartLab) using Cu K_α radiation. All the patterns were recorded at a slower rate of and with a lower step size to get a high signal to noise ratio. The structural information was derived from Rietveld refinement using the General Structure Analysis System (GSAS) software suite.[1] The visualization system for electronic and structural analysis (VESTA) program was used to draw the crystal structures.[2] The phase fractions of the dual-phase hybrid NCs were estimated using Rietveld refinement of XRD results considering full refinement of crystallographic and instrumental parameters as implemented in the GSAS program suite. Recording the low and high-resolution TEM images and Energy dispersive X-ray (EDX) analysis were performed employing JEM 2100F, using a field emission gun (FEG) at an accelerating voltage of 200 kV at Hanyang university, Seoul, South Korea. Samples for TEM were prepared by adding a solution of the nanocrystals dissolved in hexane dropwise on carbon coated Cu grid. The solution was allowed to evaporate leaving behind the nanocrystals. It is worth mentioning that cesium lead halide NCs were not stable under irradiation with high-energy electron beams for long durations. UV-visible electronic absorption spectra of various aliquots dissolved in hexane were obtained using Optizen Pop-S UV-visible spectrometer. Steady-state PL spectra of the NC/n-hexane solutions were collected using a Hitachi F-7000 fluorescence spectrophotometer. The PL lifetime measurements were carried out on the FLSP920 spectrometer, Edinburgh Instruments at Korea Advanced Institute of Science and Technology (KAIST), Seoul, South Korea. A laser was used as excitation source (λ_{ex} = 470 nm). Confocal microscopy images of the red-emitting hybrid NCs were recorded on Leica TCS SP5 by

exciting them at 458 nm and the emission collected near its maximum wavelength. The absolute PL QYs (λ_{ex} = 440 nm) of the hybrid NCs were measured in an integrated sphere (Bio-rad/C10027/C9920-20), at Korea Photonics Technology Institute, Gwangju, Seoul. The absolute PL QY values of $CsPbI_3$-Cs_4PbI_6 and $CsPbBr_3$-Cs_4PbBr_6 hybrid NCs are 75–87% and ~60%, respectively.

The variation of PL intensity during the heating-cooling cycles were measured using a connection to a Hitachi F-7000 fluorescence spectrometer with an integrated heater, temperature controller, and thermal sensor. For temperature-dependent phase stability studies, $CsPbI_3$-Cs_4PbI_6 NC films were annealed at 80^{o}C and 110^{o}C on a hot plate in the ambient air, light, and oxygen. We made sure that the NC films were in good contact with the hot plate throughout the heating process. The NC films were immersed in petri dishes filled with water for performing the water stability experiments. Usually, thin films were obtained by drop-casting of concentrated solutions of the NCs onto glass substrates.

Prototype red and green LED devices were fabricated by integrating the $CsPbI_3$-Cs_4PbI_6 and $CsPbBr_3$-Cs_4PbBr_6 hybrid NCs on a near UV LED chip (λ_{max} = 395 nm). The devices were then encapsulated in a phosphor/silicone resin mixture, followed by curing it for one hour.

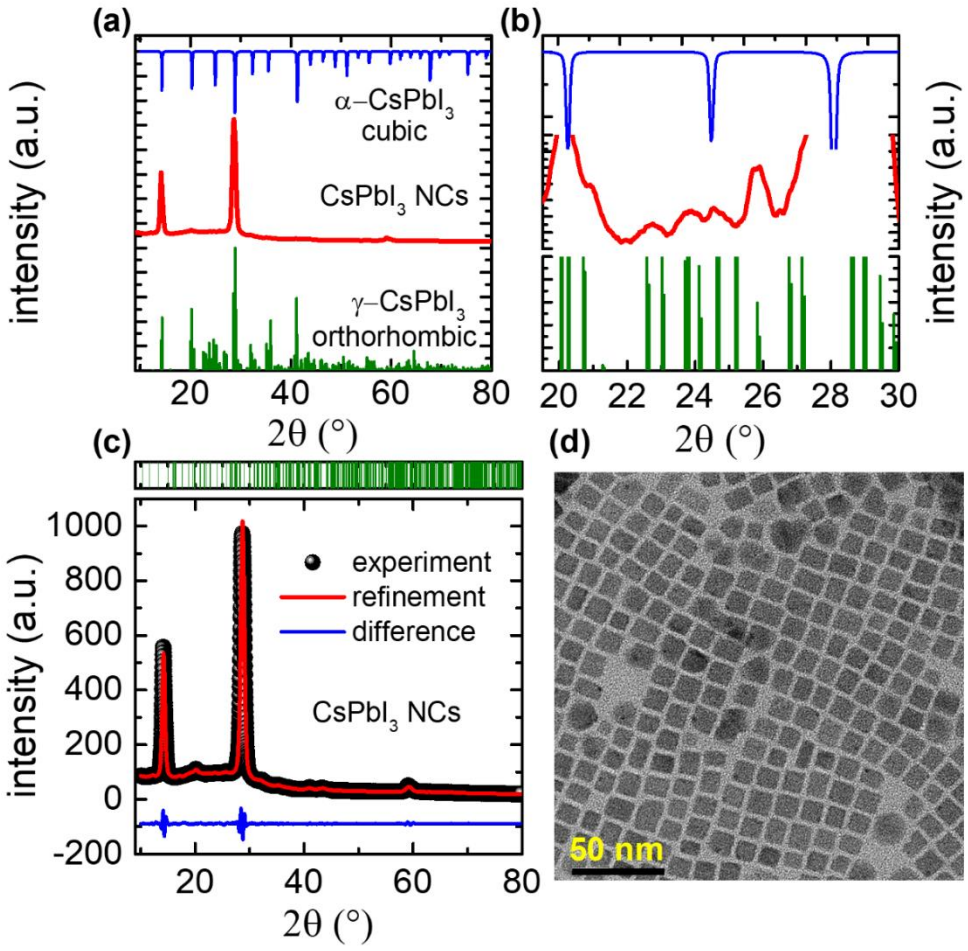

Figure S1. Structural characterization of $CsPbI_3$ NCs. (a) The XRD pattern of $CsPbI_3$ NC film together with the simulated patterns (extracted from crystallographic information file (cif)) of α-$CsPbI_3$ and γ-$CsPbI_3$. (b) is highlighting a portion of the panel (a). (c) Experimental (black dots), refined (red line), and difference (blue line) profiles obtained after full-pattern Rietveld refinement of the $CsPbI_3$ NC XRD pattern. The refined structural parameters are given in Table 1 of the main article. (d) TEM image of the NCs.

The XRD patterns α- and γ-$CsPbI_3$ have similar major reflections, as shown in Figure S4a. So, low-resolution $CsPbI_3$ NC XRD patterns can be assigned to both the phases (Figure S4a). Nevertheless, the high-resolution XRD pattern of $CsPbI_3$ NC film exhibited a few low intense reflections between 22–28º, which matches well with orthorhombic γ-$CsPbI_3$ rather than cubic α-$CsPbI_3$, as shown in Figure S4b. Furthermore, Rietveld refinement on experimentally obtained $CsPbI_3$ NC XRD pattern confirmed that the experimental data converged with the γ-$CsPbI_3$ phase.

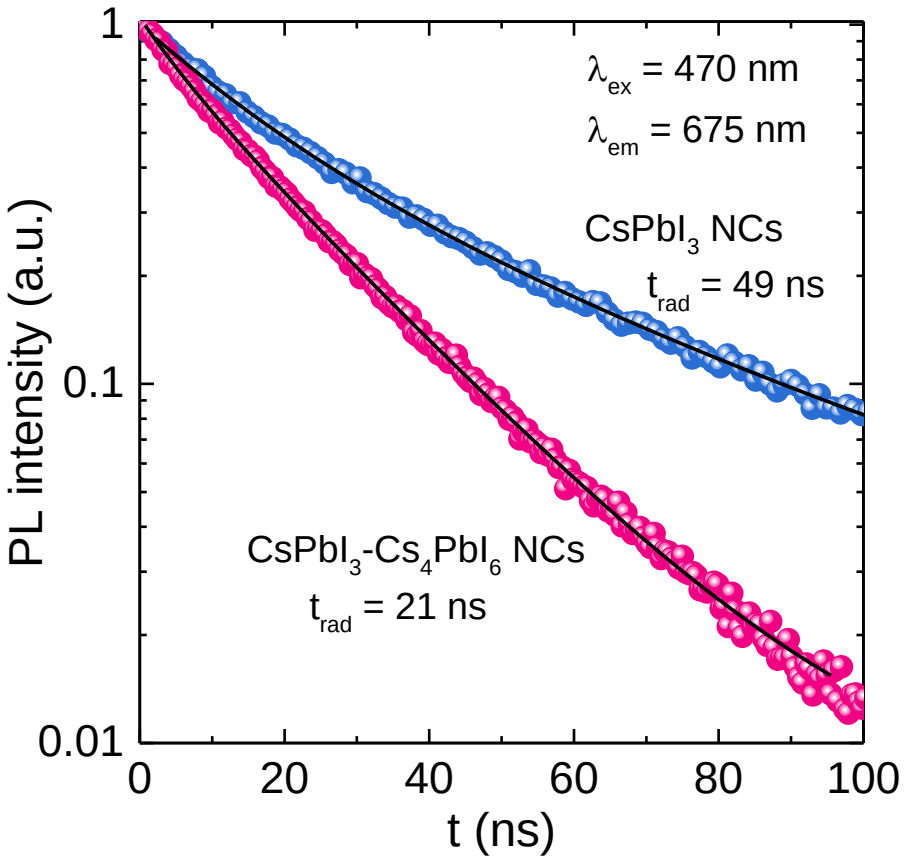

Figure S2. Time-resolved PL (TrPL) spectra of pure $CsPbI_3$ and $CsPbI_3$-Cs_4PbI_6 hybrid NCs. The scattered plots are the experimental data, and the solid lines are the corresponding bi-exponential fits. The hybrid NCs exhibit a shorter PL decay time (21 ns), and the decay profile is dominated by the radiative component (see Table S3). The PL decay characteristics of pure $CsPbI_3$ NCs matches that of the reported in the literature.[3]

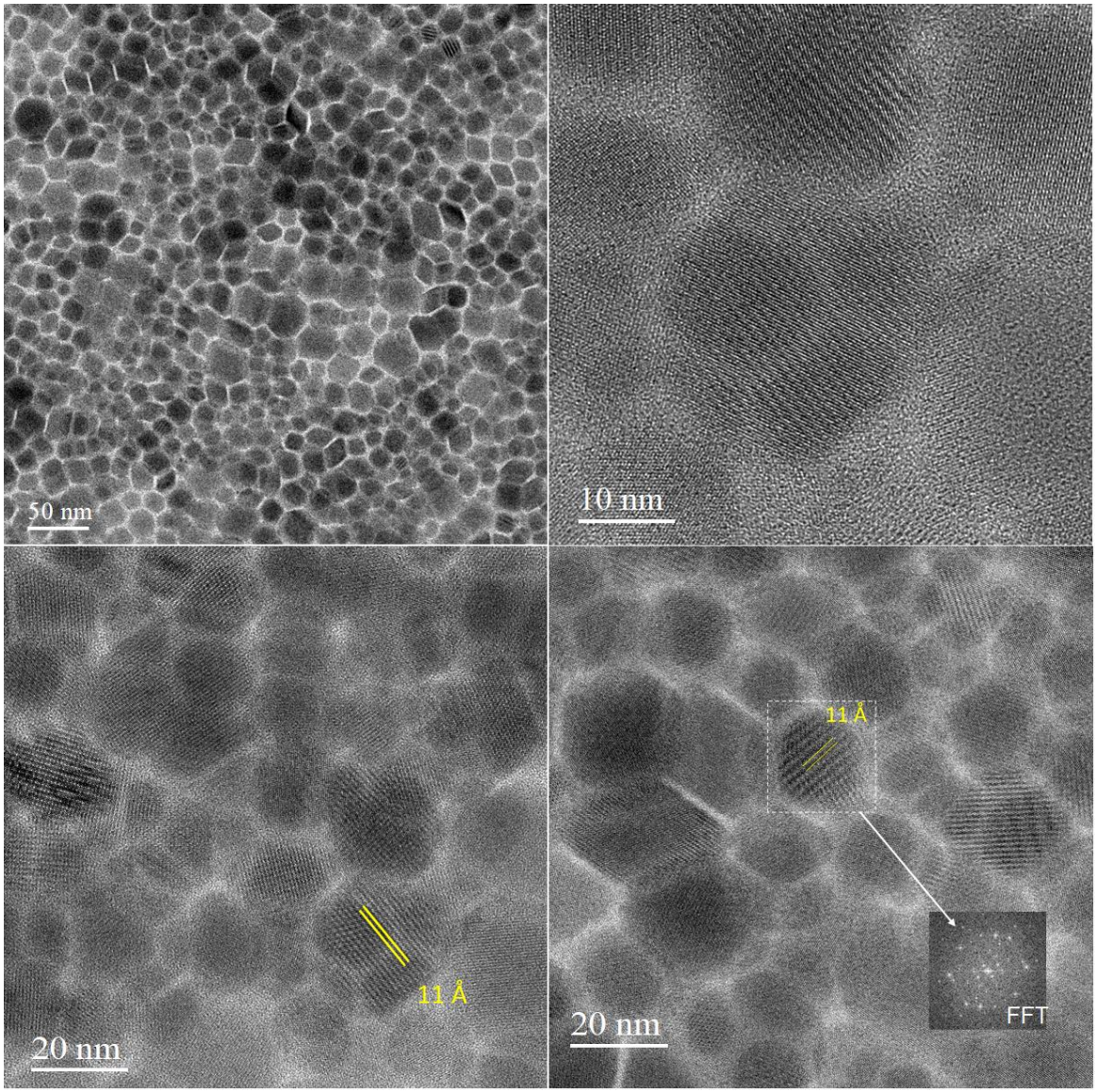

Figure S3. Additional TEM images of the $CsPbI_3$-Cs_4PbI_6 hybrid NCs. The TEM images show particles with Moiré fringe pattern (11 Å) and the ones encapsulating smaller particles as well.

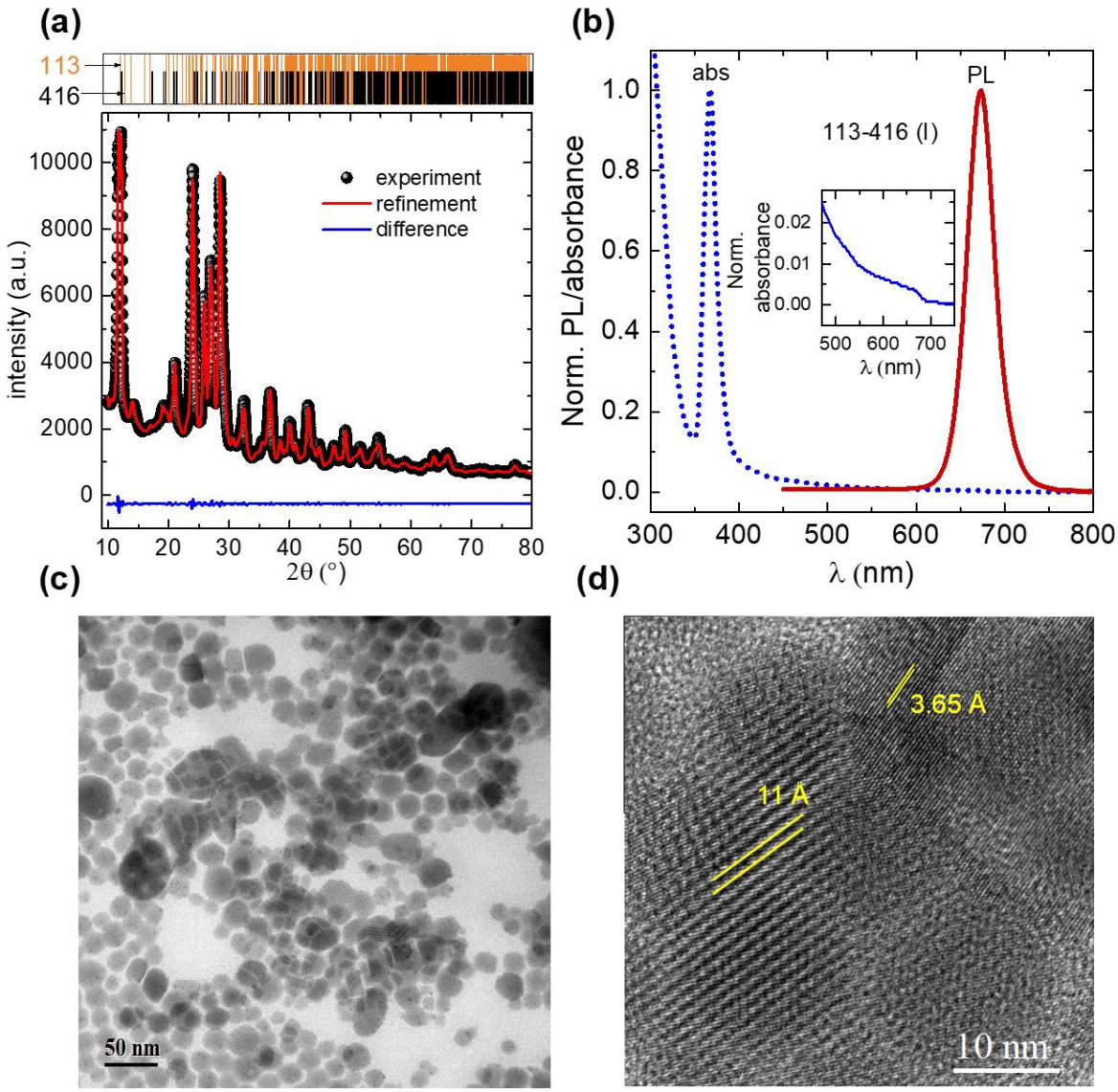

Figure S4. Structural and optical characterization of $CsPbI_3$-Cs_4PbI_6 (113-416) hybrid NCs containing 6% $CsPbI_3$ phase fraction. (a) Experimental (black dots), refined (red line), and difference (blue line) profiles obtained after full-pattern Rietveld refinement of the hybrid NC XRD pattern. (b) Electronic absorption and PL spectra of the NCs. Inset shows the absorption band correspond to the $CsPbI_3$ phase. (c) and (d) are the low and high-resolution TEM images of the NCs. 3.65 Å and 11 Å lattice spacing corresponds to the Cs_4PbI_6 phase and the Moiré fringes, respectively.

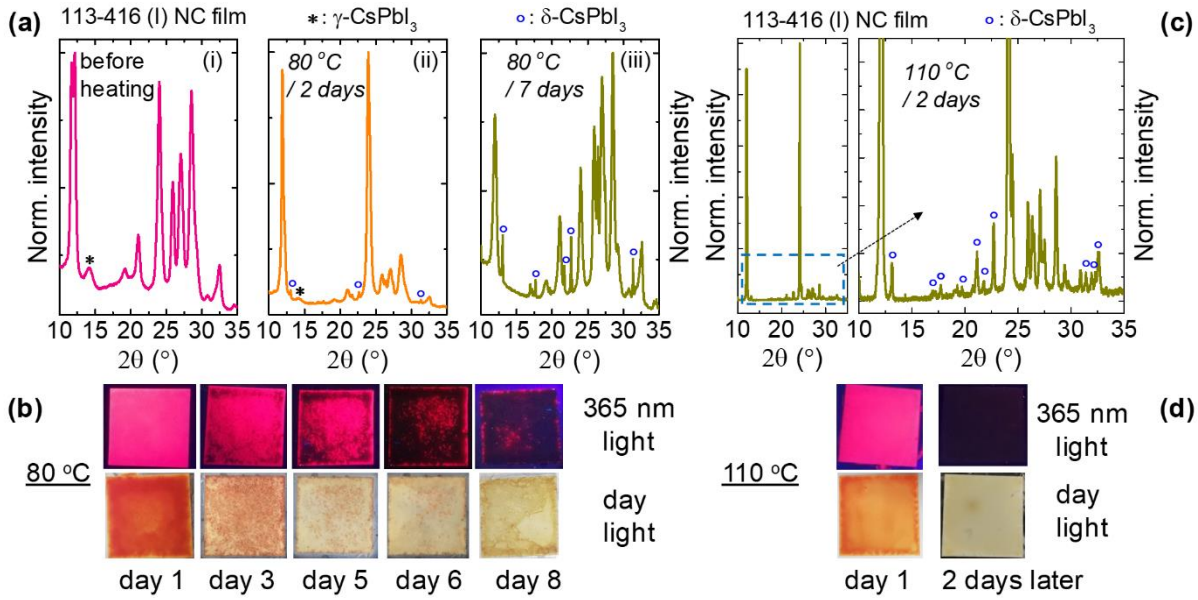

Figure S5. Phase transformation of $CsPbI_3$-Cs_4PbI_6 (113-416) NCs at elevated temperatures. (a) The XRD pattern of NC film (i) before annealing, (ii) after annealing for two days and (iii) after annealing for a week at 80°C. (b) The photographs of the NC film under room light (top) and 365 nm light (bottom) as a function of storage time at 80°C in the ambient atmosphere. (c) XRD pattern of NC film after annealing for two days at 110°C. (d) The photographs of the NC film under room light (top) and 365 nm light (bottom) stored at 110°C in the ambient atmosphere for two days.

The NC film initially consists $CsPbI_3$ in only γ-phase, a mixture of γ- and δ-$CsPbI_3$ phases appeared after annealing for two days at 80°C and all the and γ-$CsPbI_3$ converted into δ-$CsPbI_3$ after annealing the NC film at 80°C for a week. Therefore, the $CsPbI_3$ NCs embedded within Cs_4PbI_6 NC matrix gradually converted from the luminescent γ-phase into the non-luminescent δ-$CsPbI_3$ phase within a week at 80°C atmosphere. Furthermore, the phase transformation was accelerated when the NC film was kept at 110°C.

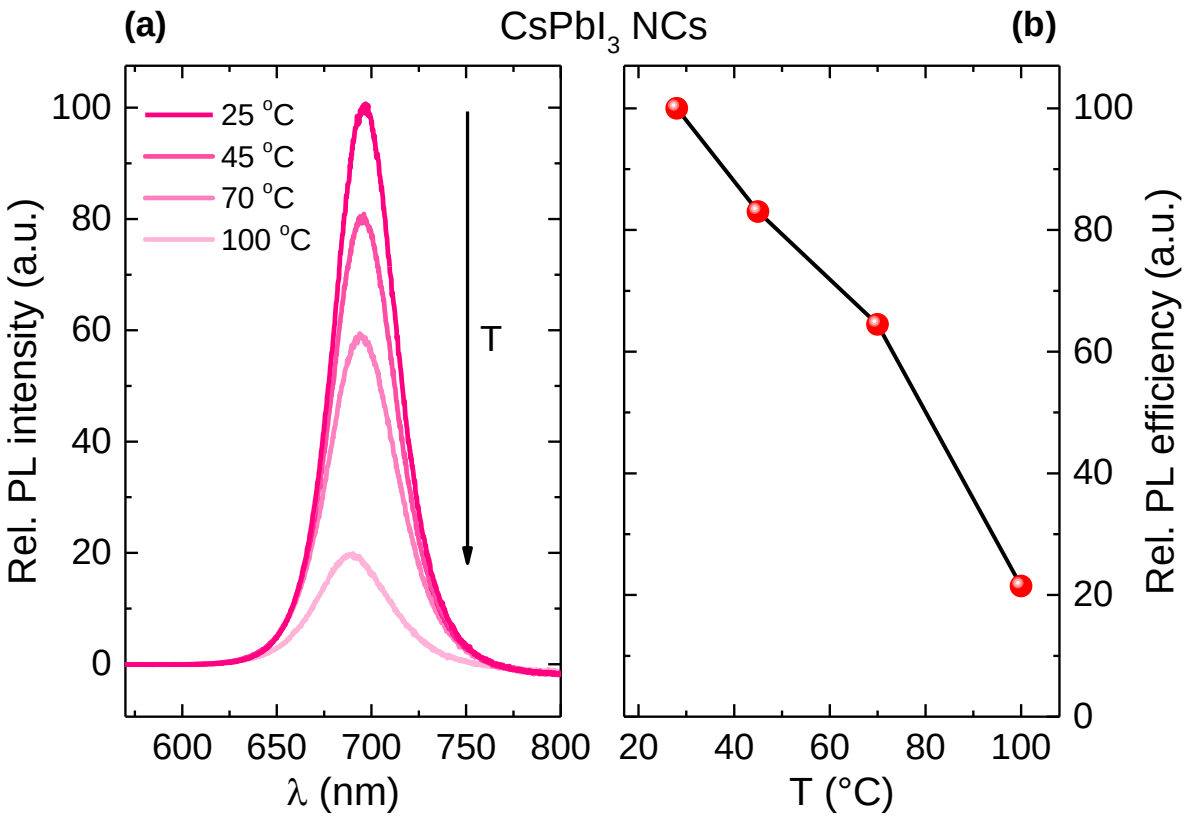

Figure S6. PL thermal quenching behavior of $CsPbI_3$ NCs. (a) PL spectra of the NCs as function of temperature and (b) is the corresponding variation of the relative PL efficiency.

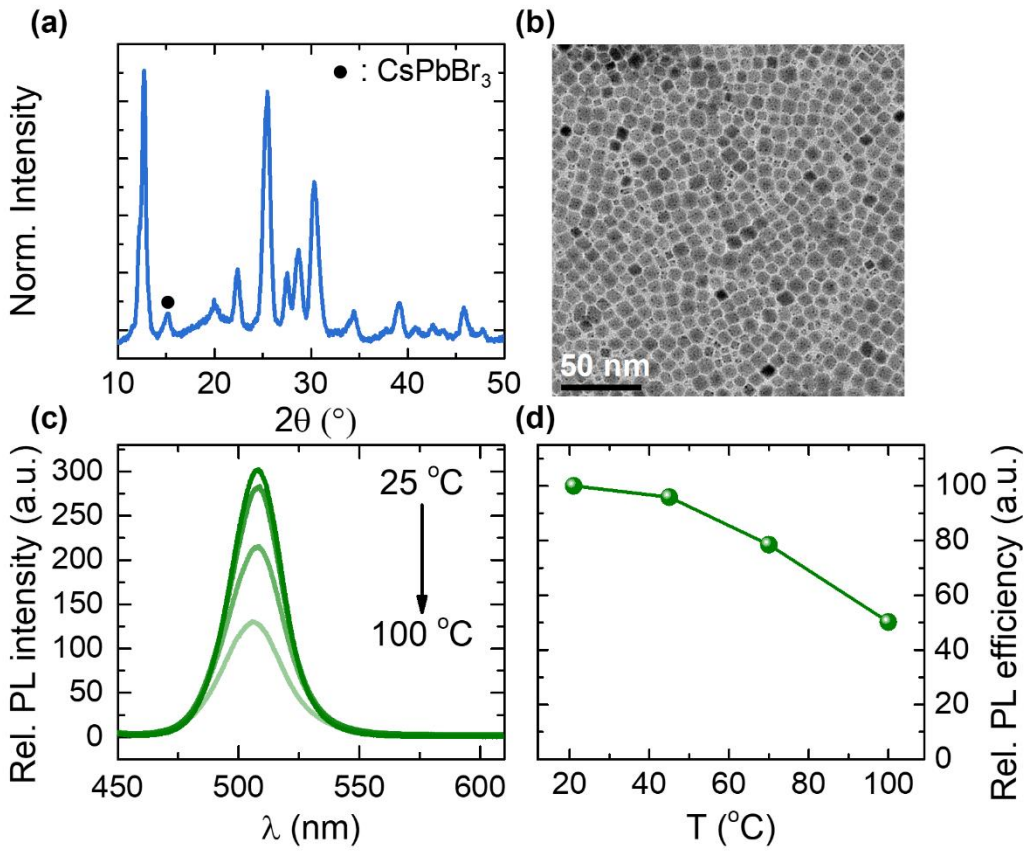

Figure S7. (a) and (b) are the XRD pattern and TEM image of green-emitting $CsPbBr_3$-Cs_4PbBr_6 hybrid NCs. (c) PL spectra of the NCs as function of temperature and (d) is the corresponding variation of the relative PL efficiency.

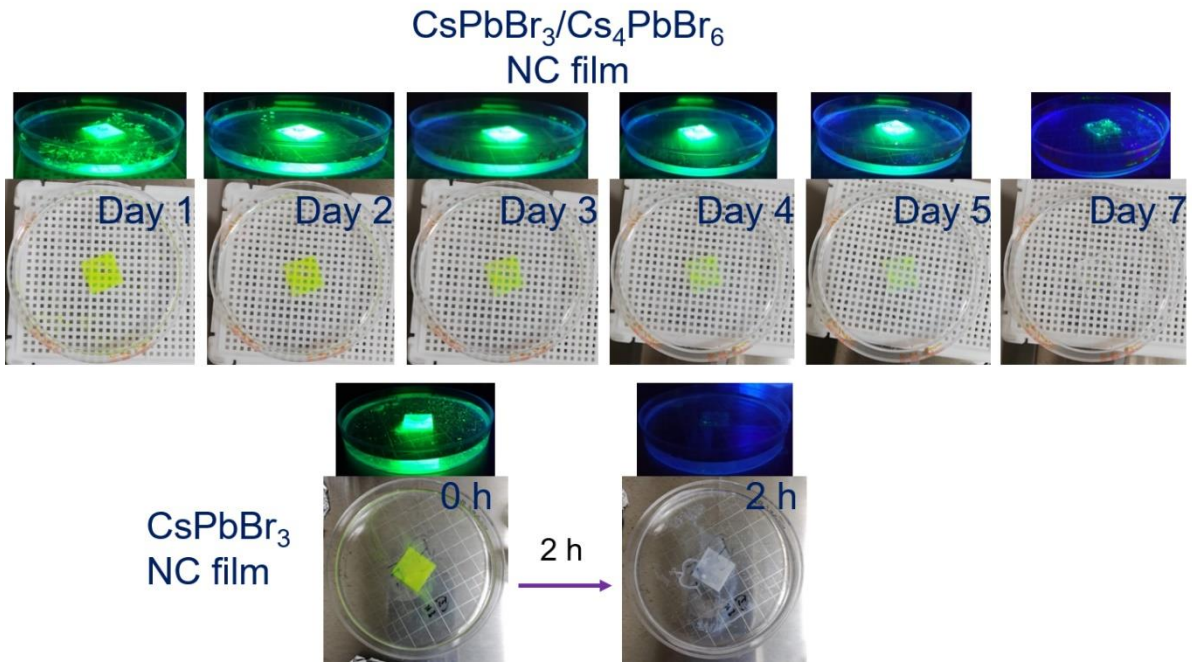

Figure S8. The improved aqueous stability of green-emitting $CsPbBr_3$-Cs_4PbBr_6 NC films. The hybrid NC films were dissolved in water after seven days of immersion whereas pure $CsPbBr_3$ NC films took just two hours for the same.

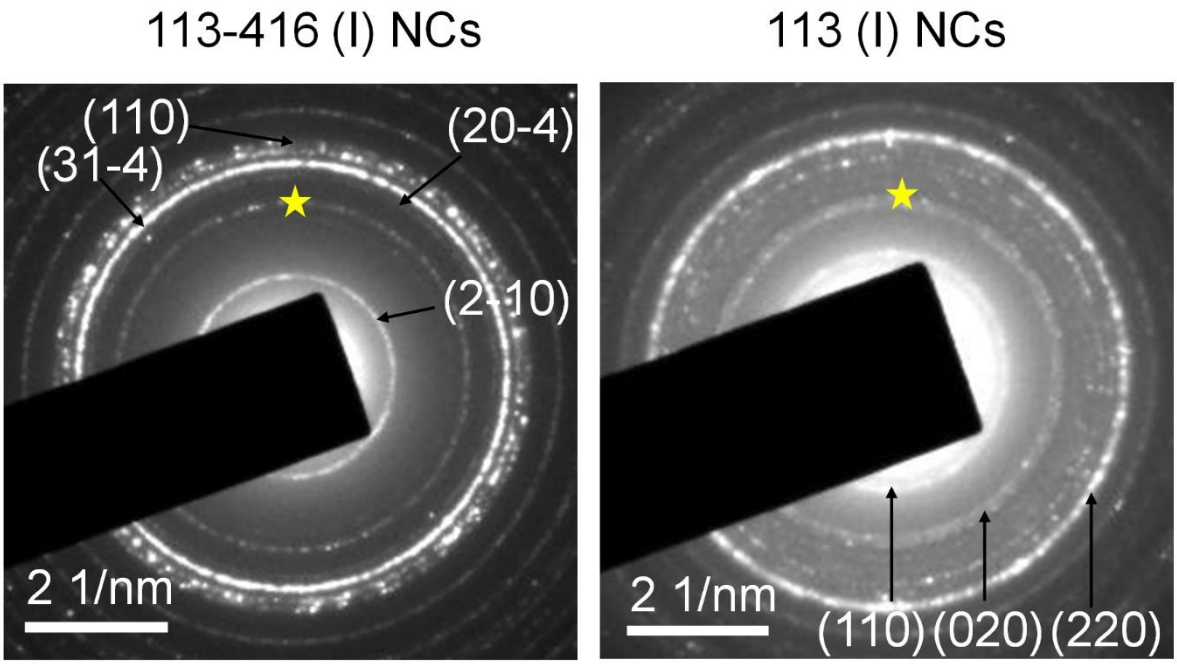

Figure S9. The electron diffraction pattern and the indexing of the lattice planes (or diffraction rings) of $CsPbI_3$-Cs_4PbI_6 (113-416) NCs (left) and pure $CsPbI_3$ NCs (right), respectively. The spacing of the (020) plane of pure $CsPbI_3$ NCs, which is marked with the asterisk symbol is close to that of the lattice plane of the hybrid NCs marked with the same symbol.

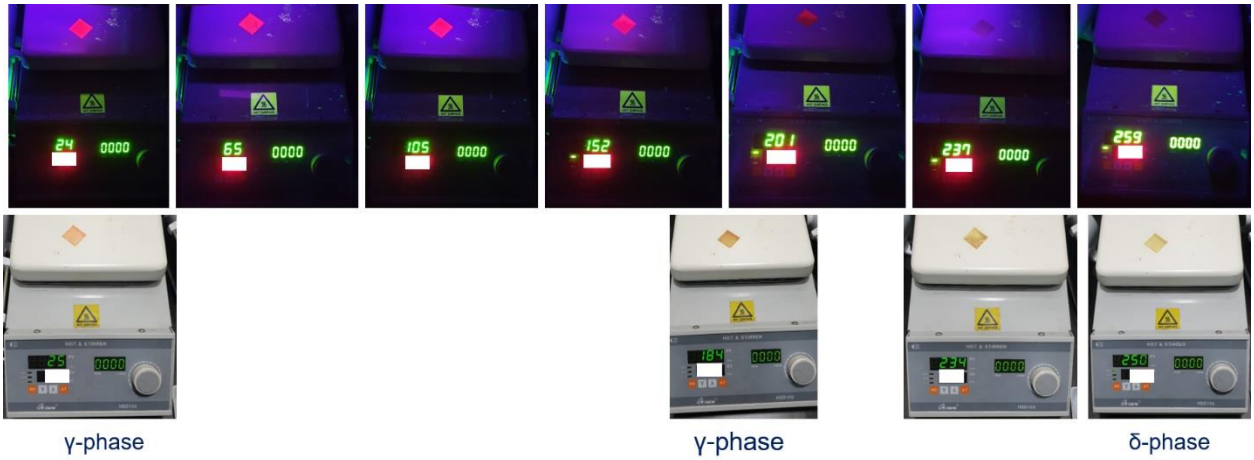

Figure S10. The photographs of the $CsPbI_3$-Cs_4PbI_6 hybrid films placed on a hot plate under UV (365 nm) light (top) and under room light (bottom). The red emission remains brighter until 150^{o}C and gets quenched above 200^{o}C. The color of the films started turning into yellow above 200^{o}C and completely turned into yellow (suggesting transformation from γ-phase to δ-phase) above 250^{o}C.

Table S1. Lattice parameters of Cs_4PbI_6 and γ-$CsPbI_3$ NCs obtained by performing Rietveld refinement on the experimental $CsPbI_3$-Cs_4PbI_6 hybrid NC XRD pattern. The refinement was performed by considering only the Cs_4PbI_6 phase (first case) and by including both Cs_4PbI_6 and γ-$CsPbI_3$ phases (second case), on the same diffraction pattern. The χ^2 (goodness of the fit) is minimal when dual phases were considered.

phase	space group	*a* (Å)	*b* (Å)	*c* (Å)	*V* (Å)^3	*Z*	R_{wp}(%)	χ^2	phase fraction (%)
Cs_4PbI_6	*R -3 c*	13.72(6)	13.72(6)	17.30(11)	2821(2)	4	17.3	*14.23*	100.00
γ-$CsPbI_3$+	*P n a m*	8.94(4)	8.76(4)	12.70(9)	965(2)	4	5.3	*3.03*	1.50
Cs_4PbI_6	*R -3 c*	14.53(9)	14.53(9)	18.27(7)	3340(5)	6			98.50

Note: The numbers in parentheses are the estimated standard deviations of the last significant figure.

Table S2. Structural parameters obtained for (a) γ-$CsPbI_3$ and (b) Cs_4PbI_6 phases on performing Rietveld refinement on NC film XRD patterns at room temperature. The numbers in parentheses are the estimated standard deviations of the last significant figure.

(a) γ-$CsPbI_3$

atom	Wyckoff position	*x*	*y*	*z*	100xU_{iso}(Å)^2
Cs	4*c*	0.4599(1)	0.5050(7)	0.2500(3)	0.0126(7)
Pb	4*b*	0.0000(0)	0.5000(0)	0.0000(0)	0.0126(0)
I	4*c*	0.0011(3)	0.6244(2)	0.2500(7)	0.2322(5)
I	8*d*	0.3225(7)	0.6304(3)	-0.0312(5)	0.0440(3)

(b) Cs_4PbI_6

Atom	Wyckoff position	*x*	*y*	*z*	100xU_{iso}(Å)^2
Cs	6*a*	0.0000(0)	0.0000(0)	0.2500(0)	0.0792(5)
Cs	18*e*	-0.2916(7)	-0.3300(4)	-0.0830(2)	0.0210(3)
Pb	6*b*	0.0000(0)	0.0000(0)	0.0000(0)	0.0481(6)
I	36*f*	0.0280(3)	-0.1600(2)	-0.1069(7)	0.0837(11)

Table S3. The PL decay parameters obtained by fitting the TrPL spectra in Figure S2 to bi-exponential decay function. While t_{slow} and t_{fast} represent the lifetime values of slower and faster decay components of the TrPL spectra, respectively, their respective percentage contributions are given as A_{slow} and A_{fast}.

	t_{slow} (ns)	A_{slow} (%)	t_{fast} (ns)	A_{fast} (%)
$CsPbI_3$ NCs	49	50	16	50
$CsPbI_3$-Cs_4PbI_6 NCs	21	82	06	18

Table S4. The atomic composition of the $CsPbI_3$-Cs_4PbI_6 hybrid NCs determined by X-ray photoelectron spectroscopy (XPS).

atom	Cs	Pb	I
composition	3.2	1.0	2.0

One of the reasons for the large deviation of iodine composition might be the iodine defects present on the surface of the Cs_4PbI_6 matrix, which in turn, reduces the amount of iodine recorded by XPS, a surface-sensitive technique.

References

(1) Toby, B. H. EXPGUI, a graphical user interface for GSAS. *J. Appl. Crystallogr.* **2001,** *34*, 210-213.

(2) Momma, K.; Izumi, F. VESTA: a three-dimensional visualization system for electronic and structural analysis. *J. Appl. Crystallogr.* **2008,** *41*, 653-658.

(3) Shi, J.; Li, F.; Yuan, J.; Ling, X.; Zhou, S.; Qian, Y.; Ma, W. Efficient and stable $CsPbI_3$ perovskite quantum dots enabled by in situ ytterbium doping for photovoltaic applications. *J. Mater. Chem. A* **2019,** *7*, 20936-20944.